

A Monte Carlo simulation of the interactions of cosmic rays with the atmosphere

P. Zuccon¹, B. Bertucci¹, B. Alpat¹, R. Battiston¹, G. Battistoni², W. J. Burger¹, G. Esposito¹, A. Ferrari^{2,3}, E. Fiandrini¹, G. Lamanna¹, and P. Sala^{2,3}

¹Università and Sezione INFN of Perugia, Italy

²Sezione INFN of Milano, Italy

³ CERN Switzerland

Abstract. Substantial fluxes of protons and leptons with energies below the geomagnetic cutoff have been measured by the AMS experiment at altitudes of 370-390 Km, in the latitude interval $\pm 51.7^\circ$. The production mechanisms of the observed trapped fluxes are investigated in detail by means of the FLUKA Monte Carlo simulation code. All known processes involved in the interaction of the cosmic rays with the atmosphere (detailed descriptions of the magnetic field and atmospheric density, as well as the electromagnetic and nuclear interaction processes) are included in the simulation. The results are presented and compared with the experimental data, indicating good agreement with the observed fluxes.

1 Introduction

Cosmic rays approaching the earth interact with the atmosphere resulting in a substantial flux of secondary particles. A reliable estimate of the secondary flux composition and energy spectra is of great interest for different reasons, as for example the evaluation of background radiation for satellites or the estimate of the atmospheric neutrino production for neutrino oscillation experiments, see for example (G. Battistoni, 2000) that made use of the same interaction model used in this work.

The accurate AMS measurements of charged fluxes of cosmic and secondary particles in the near Earth region allow to perform an extensive test of models describing the cosmic ray interactions with the atmosphere and the evolution of the produced secondary particles in the magnetic field.

In this work we report on a Monte Carlo simulation that describes the interactions of cosmic protons with the Earth's atmosphere, following all secondaries in their motion in the Earth's magnetic field.

2 The model

An isotropic flux of protons is uniformly generated on a geocentric spherical surface with a radius of 1.07 Earth radii ($\sim 500\text{Km}$ a.s.l.) in the kinetic energy range $0.1 - 170\text{GeV}$.

The energy spectrum is modeled according to a power law, modified to account for the solar modulation effects as suggested in (Gleeson and Axford, 1968). Both the spectral index and the solar modulation parameter are extracted from a fit to the AMS data (AMS Collaboration, 2000-b).

The magnetic field in the Earth's proximity is obtained summing two components: the Earth's magnetic field, calculated using a 10 harmonics IGRF (Tsyganenko, 1992) implementation, and the external magnetic field, calculated using the Tsyganenko Model¹ (Tsyganenko, 1996).

To account for geomagnetic effects we backtrace each primary proton until one of the following conditions is satisfied:

1. the particle reaches the distance of $10E_R$ from the Earth's center.
2. the particle touches again the production sphere.
3. neither 1 or 2 is satisfied before a time limit is reached.

If condition 1 is satisfied the particle is on an allowed trajectory, while if condition 2 is satisfied the particle is on a forbidden one. Condition 3 arises for only a small fraction of the events (0.0001 %).

Particles on allowed trajectories are propagated forward and can reach the Earth's atmosphere. The atmosphere around the Earth is simulated up to 120Km a.s.l. using 60 concentric layers of homogeneous density and chemical composition. Data on density and chemical composition are taken from the standard MSIS model (A. E. Hedin, 1991). The Earth is modeled as a solid sphere absorbing each particle reaching its surface.

¹The external magnetic field is calculated only for distances greater than 2 Earth's radii (E_R) from the Earth's center

2.1 The interaction model

We use the software package FLUKA 2000 (A. Ferrari et al., 2000) to transport the particles and describe their interactions with Earth's atmosphere. This package is tri-dimensional and should reproduce the spatial distribution of secondaries better than older models based on empirical parameterizations of accelerator data.

Interactions are treated in a theory-driven approach, and the models and their implementations are always guided and checked using experimental data. Hadron-nucleon interaction models are based on resonance production and decay below a few GeV and on the Dual Parton Model above.

The extension to hadron-nucleus interactions is done in the framework of a generalized intra-nuclear cascade approach including the Gribov-Glauber multi-collision mechanism for higher energies followed by equilibrium processes: evaporation, fission, Fermi break-up, and γ De-excitation.

In fig 1 a) we show the map of the primary proton interaction points in geographical coordinates. The distribution reflects the influence of the geomagnetic cutoff. Fig 1 b) shows the interactions altitude profile, the solid histogram is for $E_k < 30 GeV$ while the dashed one is for $E_k > 30 GeV$. The mean interaction altitude depends weakly on the energy.

In tab.1 we show the characteristic features of the cosmic proton interactions in the atmosphere.

	$E_k < 30 GeV$	$E_k > 30 GeV$
Elastic interactions	26%	24%
Inelastic interactions	74%	76%
Multiplicity of secondaries	5	11

Table 1. Characteristics of the cosmic protons interactions with atmosphere

3 Comparison with the AMS data

To compare with the AMS data we describe the “detector” as a spherical surface corresponding to the AMS orbit ($400Km$ a.s.l) and we record each particle that crosses the detection boundary with an angle with respect to the zenith (or nadir) direction within the AMS field of view.

To obtain the absolute normalization, we take into account the field of view, the corresponding AMS acceptance, and an equivalent time exposure (E.T.E) corresponding to the number of primary protons generated.

Our results are based on a sample of $\sim 3 \cdot 10^6$ primary protons generated in the kinetic energy range of $0.1 - 170 GeV$, which corresponds to $\sim 1 \cdot 10^{-12}s$ (E.T.E).

3.1 Protons

In fig.2, we show the comparison between the fluxes obtained with the simulation and the measured AMS downgoing proton flux (AMS Collaboration, 2000-a) in nine bins of geo-

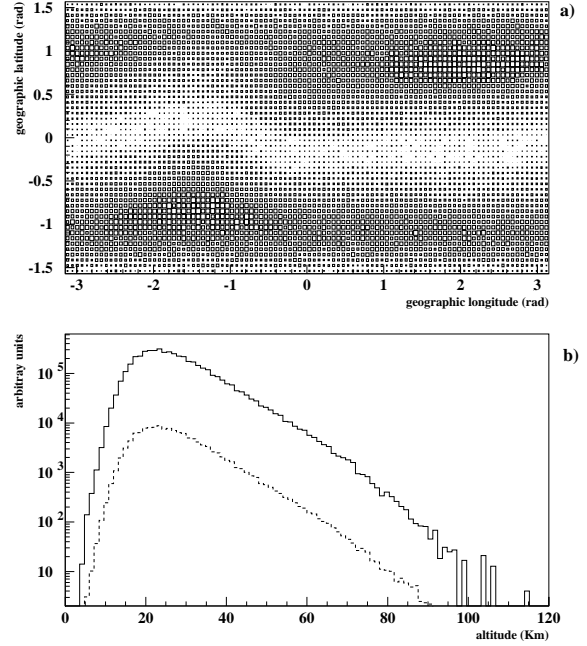


Fig. 1. a) foot-print map of primary protons interaction points in geographical coordinates, b) altitude profile of primary protons interaction points, solid line $E_k < 30 GeV$, dashed line $E_k > 30 GeV$

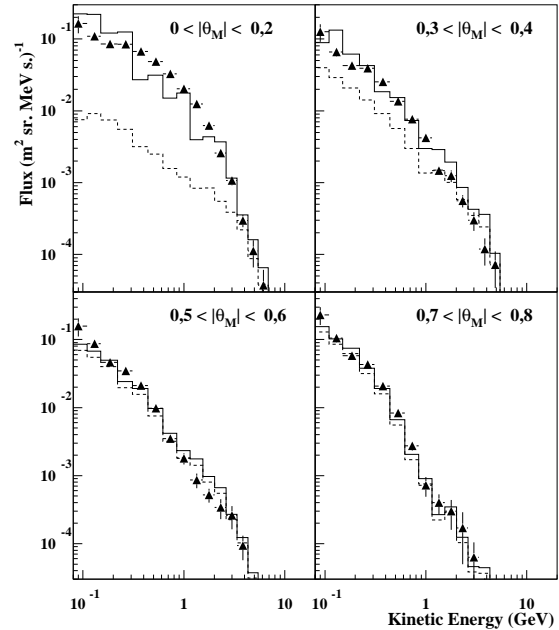


Fig. 3. Upgoing proton fluxes, simulation (solid line) and the AMS data (triangles); the dashed lines are described in the text.

magnetic latitude(θ_M). Fig.3 shows the same comparison for the upgoing proton flux in four selected θ_M bins.

As seen in fig.2 the simulation reproduces well, and for all latitudes, the high energy part of the spectrum and the falloff in the primary spectrum due to the geomagnetic cutoff, thus

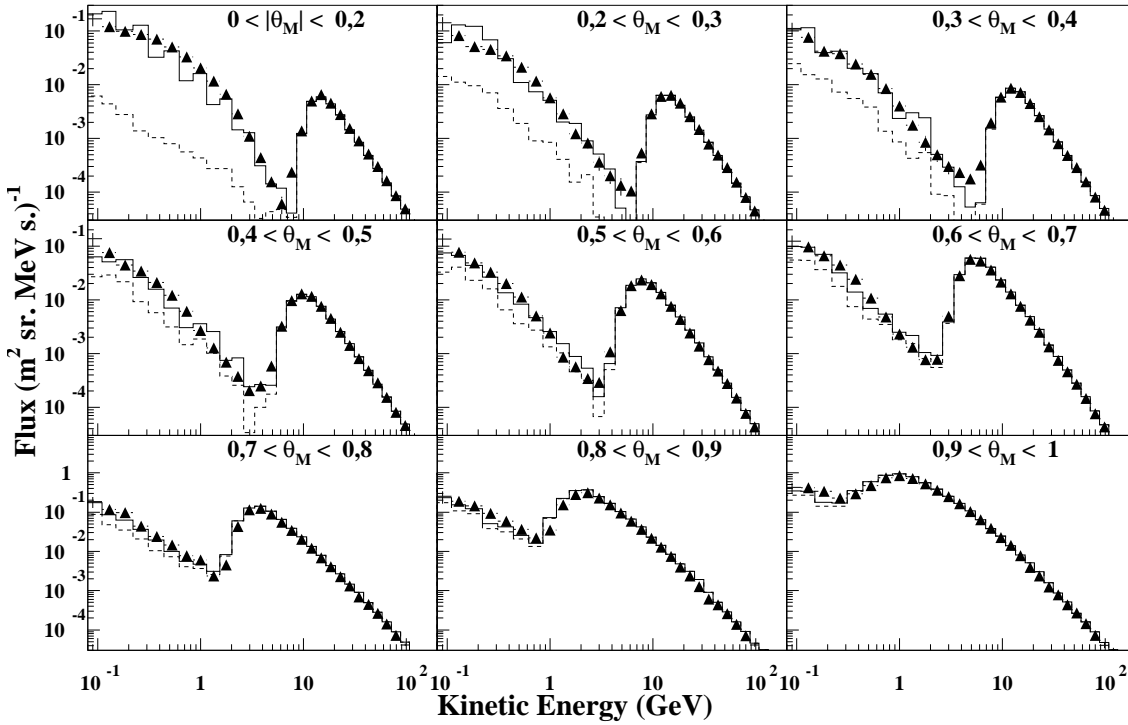


Fig. 2. Downgoing proton flux, simulation(solid line) and the AMS data (triangles); the dashed lines are described in the text.

validating the general approach used for the generation and detection, as well as the tracing technique.

The part of the spectrum below the geomagnetic cutoff is sensitive to the interaction model used; the results shown in figs. 2 and 3 were obtained with FLUKA2000(A. Ferrari et al., 2000).

In figs. 2 and 3 bin-to-bin statistical fluctuations are seen at the lower kinetic energies, particularly in the equatorial region. This part of the spectrum corresponds to the undercutoff component where the observed flux is the result of multiple detections of the same particles. The importance of this effect on the observed fluxes is illustrated by the *real proton flux*, i.e. the flux obtained by counting only once each particle crossing the detector, which is indicated by the dashed distributions in figs. 2 and 3. In particular, the *real number* of protons crossing the detector in the equatorial region is more than one order of magnitude lower than the observed flux. As a consequence, for the simulated results, statistical fluctuations are amplified by this effect. At high geomagnetic latitudes, the solid and dashed lines merge. The effect becomes negligible for $\theta_M > 0.8$.

Within the formalism of adiabatic invariants, it is seen that trapped particles, i.e. the undercutoff protons, move along drift shells which can be associated with a characteristic residence time² that depends on the fraction of the shell located inside the Earth's atmosphere. Thus, particles moving along

²The mean time after which a particle is absorbed into the atmosphere.

long-lived shells have a large probability to cross many times a geocentered spherical detector, while those moving along *short-lived* shells typically cross the detector one time. The drift shells crossing the AMS orbit, at an altitude of 400 km, are in general *long-lived* in the equatorial region and *short-lived* at higher latitudes. A more detailed discussion of particle residence times can be found in (E.Fiandrini et al., 2001); the characteristics of the observed *long-lived* and *short-lived* undercutoff proton populations, and in particular the experimental confirmation of the above picture, can be found in (AMS Collaboration, 2000-a).

3.2 Electrons and positrons

In fig. 4 we show a comparison of the simulated undercutoff electron and positron downgoing fluxes with the corresponding AMS measured fluxes (AMS Collaboration, 2001-c). The AMS positron measurement is limited to energies below 3 GeV, corresponding to the upper limit of proton rejection of the threshold Cherenkov counter used to distinguish protons and positrons.

In fig.5b-c we show the integrated positron and electron downgoing fluxes for the kinetic energy range 0.2 – 1.5 GeV as a function of θ_M . The simulation reproduces reasonably well the general behavior of the experimental data in terms of shape and intensity; a similar agreement is observed for the upgoing lepton spectra (not shown).

As in the case of protons, statistical fluctuations affect the comparison in the equatorial region. The *real lepton fluxes*,

corresponding to the *real proton flux* described earlier, are shown as the dashed line distributions in fig. 4

An interesting feature which emerges from the comparison is the fact that in the equatorial region, the electrons are produced essentially by primary protons with $E_k > 30 \text{ GeV}$, while for the positrons lower energy protons contribute as well. This distinction disappears at higher latitudes.

This behavior can be explained by the GMC East-West asymmetry affecting the primary protons. Westward moving protons produce positrons which will populate the drift shells, while the produced electrons enter the atmosphere (Derome, 2001). The energy spectrum of eastward moving protons is affected by the geomagnetic cutoff. As a consequence, the protons producing electrons in the equatorial region have higher energies (lower flux) yielding a lower undercutoff electron flux compared to the undercutoff positron flux.

4 Conclusion

Our results show good agreement between simulation and the measured data. The Monte Carlo simulation describes well the undercutoff proton and lepton fluxes. The simulation, constrained by the high statistic measurements of AMS can be used to assess the radiation environment in near-Earth orbit, and provides new constraints for calculations of atmospheric neutrino production.

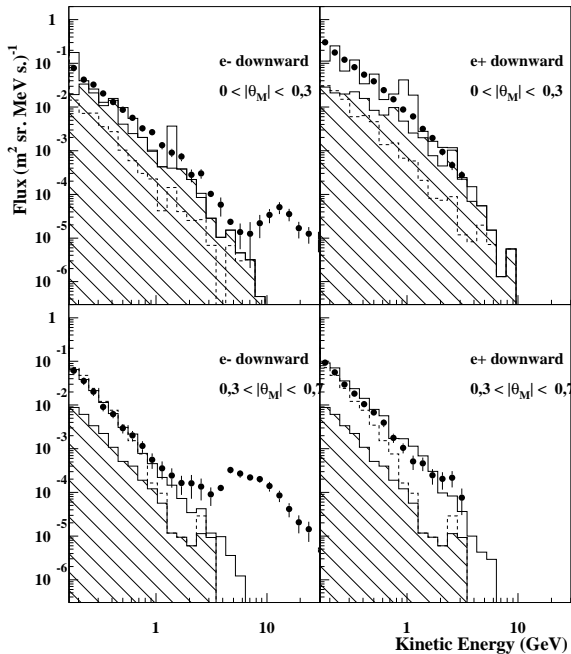


Fig. 4. Downgoing positron and electron fluxes in two regions of geomagnetic latitude θ_M , solid histogram (simulation) black points (AMS data); hatched histogram shows the positron and electron fluxes produced by primary protons with $E_k > 30 \text{ GeV}$; the dashed line distributions are described in the text.

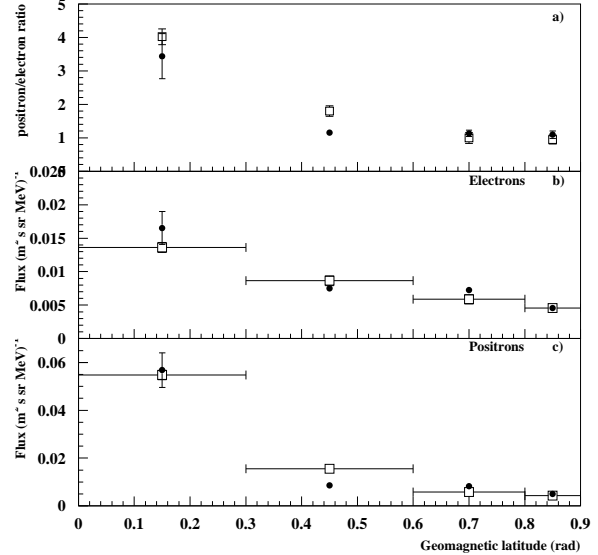


Fig. 5. Electron (b) and positron (c) fluxes and their ratio (a) integrated in the kinetic energy range $0.2 - 1.5 \text{ GeV}$, as function of geomagnetic latitude. Open squares (AMS data), black points (simulation).

This work has been partially supported by the Italian Space Agency (ASI) under contract ARS-98/47.

References

- J.Alcaraz et al.,AMS Collaboration, Protons in Near Earth Orbit, Phys.Lett. B472, 215-226, 2000 (a).
- J.Alcaraz et al.,AMS Collaboration, Cosmic Protons, Phys. Lett. B490, 27-35, 2000 (b)
- J.Alcaraz et al.,AMS Collaboration, Leptons in Near Earth Orbit, Phys.Lett. B484, 10-22, 2000 (c).
- G. Battistoni et al., Astroparticle Physics 12,315-333, 2000.
- L.Derome et al., Origin of leptons in near earth orbit, astro-ph/0103474, 2001.
- A. Ferrari et al., The FLUKA radiation transport code and its use for space problems, Proceedings of the "1 st International Workshop on Space Radiation Research and 11 th Annual NASA Space Radiation Health Investigators' Workshop", Arona (Italy), May 27-31, 2000, Physica Medica, VOI XVII, Suppl. 1.
- E. Fiandrini, G. Esposito, B. Bertucci et al. 'Leptons with $E > 200 \text{ MeV}$ trapped in the Earth's radiation belts', ICRC 2001 proceedings.
- L.J. Gleeson and W.I.Axford, Astroph. Journal 154, p11011,1968
- A. E. Hedin, Extension of the MSIS Thermospheric Model into the Middle and Lower Atmosphere, J. Geophys. Res. 96, 1159, 1991.
- P.Lipari, The fluxes of subcutoff particles detected by AMS, the cosmic ray albedo and atmospheric neutrinos, astro-ph/0101559, 2001.
- N.A. Tsyganenko Geomagn. and Aeronomy (1986), V.26, P.523-525; N.A. Tsyganenko and M.Peredo, Geopack Manual,(1992)
- N.A. Tsyganenko and D.P. Stern, A new-generation global magnetosphere field model , based on spacecraft magnetometer data, ISTP newsletter, v.6, no.1, p.21, feb.1996.